ChemPubSoc Europe

DOI: 10.1002/chem.201304799

CHEMISTRY
A European Journal
Full Paper

Metal–Organic Frameworks

A Novel Bismuth-Based Metal–Organic Framework for High Volumetric Methane and Carbon Dioxide Adsorption

Mathew Savage,[a] Sihai Yang,*[a] Mikhail Suyetin,[a] Elena Bichoutskaia,[a] William Lewis,[a] Alexander J. Blake,[a] Sarah A. Barnett,[b] and Martin Schröder*[a]

Abstract: Solvothermal reaction of H_4L (L = biphenyl-3,3′,5,5′-tetracarboxylate) and $Bi(NO_3)_3{\cdot}(H_2O)_5$ in a mixture of DMF/MeCN/H_2O in the presence of piperazine and nitric acid at 100 °C for 10 h affords the solvated metal–organic polymer $[Bi_2(L)_{1.5}(H_2O)_2]{\cdot}(DMF)_{3.5}{\cdot}(H_2O)_3$ (NOTT-220-solv). A single crystal X-ray structure determination confirms that it crystallises in space group *P*2/*c* and has a neutral and non-interpenetrated structure comprising binuclear $\{Bi_2\}$ centres bridged by tetracarboxylate ligands. NOTT-220-solv shows a 3,6-connected network having a framework topology with a $\{4{\cdot}6^2\}_2\{4^2{\cdot}6^5{\cdot}8^8\}\{6^2{\cdot}8\}$ point symbol. The desolvated material NOTT-220a shows exceptionally high adsorption uptakes for CH_4 and CO_2 on a volumetric basis at moderate pressures and temperatures with a CO_2 uptake of 553 g L^{-1} (20 bar, 293 K) with a saturation uptake of 688 g L^{-1} (1 bar, 195 K). The corresponding CH_4 uptake was measured as 165 V(STP)/V (20 bar, 293 K) and 189 V(STP/V) (35 bar, 293 K) with a maximum CH_4 uptake for NOTT-220a recorded at 20 bar and 195 K to be 287 V(STP)/V, while H_2 uptake of NOTT-220a at 20 bar, 77 K is 42 g L^{-1}. These gas uptakes have been modelled by grand canonical Monte Carlo (GCMC) and density functional theory (DFT) calculations, which confirm the experimental data and give insights into the nature of the binding sites of CH_4 and CO_2 in this porous hybrid material.

Introduction

Porous metal–organic frameworks (MOFs) have attracted major research interest due to their potential in a wide range of applications, particularly in the field of gas adsorption and separation.[1] This research is of importance not only for the development of energy storage media for hydrogen (H_2) or methane (CH_4),[2] but also for the design of new carbon capture systems.[3] MOF materials exhibit three-dimensional extended structures incorporating both large accessible pore volume and high internal surface area, which are key features for high capacity gas adsorption. They are often based upon divalent late first row transition metals (e.g., Cu^{II} and Zn^{II}) and polycarboxylate ligands, and can show low framework densities (0.22–0.9 g cm^{-3}) leading to high gravimetric gas uptakes.[4] Thus, a great deal of current effort is focused on the synthesis of low density MOFs by using elongated organic ligands[4a–c] and/or light metal ions (e.g., Li,[5] Be,[6] Mg[7]), in order to maximise and enhance gas uptake capabilities.

[a] *M. Savage, Dr. S. Yang, Dr. M. Suyetin, Prof. Dr. E. Bichoutskaia, Dr. W. Lewis, Prof. Dr. A. J. Blake, Prof. Dr. M. Schröder*
School of Chemistry, University of Nottingham
University Park, Nottingham NG7 2RD (UK)
E-mail: M.Schroder@nottingham.ac.uk

[b] *S. A. Barnett*
Diamond Light Source, Harwell Science and Innovation Campus
Didcot, Oxfordshire, OX11 0DE (UK)

Supporting information for this article is available on the WWW under http://dx.doi.org/10.1002/chem.201304799; containing views of crystal structures, details of gas adsorption data and analyses, TGA, PXRD data and GCMC calculations.

Despite intense research on H_2 storage materials in recent years, no feasible storage media have been discovered to meet DoE storage capacity targets at moderate temperature and pressure.[8] Thus, as a promising alternative to H_2, CH_4 is attracting considerable interest for on-board mobile applications due to its high molar energy density and low carbon content, leading to lower carbon dioxide (CO_2) emissions by combustion.[2] However, at ambient temperatures and pressures, CH_4 has a low energy density in the gaseous phase, but this density can be increased by compression or liquefaction. Compressed natural gas requires bulky, heavy-walled storage tanks and expensive dual-stage compressors, whereas liquefaction of methane can only be achieved at cryogenic temperatures, necessitating complex tank design in order to maintain the low temperature and reduce boil-off. As a result, neither of these approaches is suitable for small, light-duty consumer automobiles.

The alternative is to use porous sorbents to store natural gas at high density at ambient temperatures and moderate pressures (typically 35 bar). Volumetric gas uptake is an important criterion if these systems are to find practical applications, because high volumetric uptake minimises the volume of storage material and therefore the size of the fuel tank. This is of critical importance as it will allow adsorbed natural gas tanks to be more optimally integrated into the limited space available within a small vehicle. Unfortunately, low-density MOFs, even those with high gravimetric gas uptake, typically have low volumetric uptakes as a consequence of their low density. Moreover, very low density MOFs with high percentage pore voids often show poor framework stability upon removal of guest solvents, resulting in the decomposition of the materi-

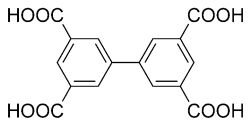

Scheme 1. View of biphenyl-3,3′,5,5′-tetracarboxylic acid (H_4L).

al.[9] We report herein the development of a unique highly porous and high density system NOTT-220-solv constructed from biphenyl-3,3′,5,5′-tetracarboxylate (L^{4-}) and Bi^{3+} ions, a metal which is rarely used in MOF construction due partly to its high density (Scheme 1).[10] NOTT-220-solv shows a new framework topology based upon binuclear {Bi_2} nodes, and the combination of a large pore void (up to 54%) and a high gas affinity leads to high volumetric uptakes in desolvated NOTT-220a at saturation: 287 V(STP)/V for CH_4 at 195 K, 20 bar; 688 g L^{-1} for CO_2 at 195 K, 1.0 bar. The experimental uptakes for CH_4 have been confirmed by modelling studies and confirm that at ambient temperatures the volumetric CH_4 uptake in NOTT-220a (189 V(STP/V) at 35 bar and 293 K) is high overall, but lower than those MOFs showing capacities greater than 200 V/(STP/V) under the same conditions such as Ni-, Co- and Mg-MOF-74,[2e,11] HKUST-1[2e] and PCN-14.[2e,12]

Experimental Section

List of materials

NOTT-220-solv: $[Bi_2(C_{16}H_6O_8)_{1.5}(H_2O)_2]\cdot(DMF)_{3.5}\cdot(H_2O)_3$ as-synthesised sample.

NOTT-220-acetone: $[Bi_2(C_{16}H_6O_8)_{1.5}(H_2O)_2]\cdot(C_3H_6O)_{2.5}\cdot(H_2O)_{4.5}$ acetone-exchanged sample.

NOTT-220a: $[Bi_2(C_{16}H_6O_8)_{1.5}]$ desolvated sample.

Synthesis of NOTT-220-solv

H_4L (Scheme 1; 15 mg, 0.045 mmol), $Bi(NO_3)_3\cdot(H_2O)_5$ (17 mg, 0.035 mmol) and piperazine (7.0 mg, 0.081 mmol) were combined in a 23 mL glass pressure tube. DMF/MeCN mixture (1.3 mL, 1:0.3 v/v) was added to the tube and the white slurry was acidified with dilute nitric acid (5%, 0.3 mL). The reaction vessel was heated to 100 °C in an oil bath for 10 h. When a white crystalline precipitate was observed, the hot reaction vessel was quickly cooled with cold water to avoid the formation of recrystallised ligand as impurities. The white crystalline powder was washed several times with DMF, and dried briefly in air. Yield: 10 mg (25%). Elemental anaylsis (%) for $[Bi_2(C_{16}H_6O_8)_{1.5}(H_2O)_2]\cdot(DMF)_{3.5}\cdot(H_2O)_3$ calcd: C 34.5, H 3.6, N 3.5; found: C 34.0, H 3.1, N 4.1. The volatility of crystallisation solvents in the samples contributes to the discrepancy in elemental analytical data. Selected IR(ATR): $\tilde{\nu}=3366$ (b) H_2O, 2928 (w) C–H, 2160 (w), 1978 (w), 1645 (s) O–H, 1539 (m) C–O, 1315 (m), 1252 (m) C–O, 1097 (m), 906 (w), 851 (w), 770 (m), 735 (s), 661 (s) cm^{-1}.

Gas adsorption isotherms

H_2, N_2, CO_2 and CH_4 isotherms (0–20 bar) were recorded at 77 K (by liquid nitrogen) or 87 K (by liquid argon), 195 K (by dry ice/acetone) or 273 and 293 K (by temperature-programmed water bath) on an IGA-003 system (Hiden Isochema, Warrington, UK) at the University of Nottingham under ultrahigh vacuum in a clean system with a diaphragm and turbo pumping system. Ultrapure plus grade (99.9995%) H_2 was purchased from BOC and purified further using calcium aluminosilicate and activated carbon adsorbents to remove trace amounts of water and other impurities before introduction into the IGA system. Research grade CH_4, CO_2 and N_2 were purchased from BOC and used as received. Powder samples were loaded into the IGA and degassed at 100 °C and 10^{-10} bar for 1 day to give desolvated samples. In a typical procedure, approximately 50 mg of dry sample was used for the measurements.

Single crystal X-ray determinations

X-ray diffraction data on single crystals of the α and β forms of NOTT-220-solv were collected at 100(2) K on a Bruker APEXII CCD area detector using graphite monochromated $Mo_{K\alpha}$ radiation from a rotating anode source at the UK National Crystallography Service at the University of Southampton, UK, and at 120(2) K on a Rigaku Saturn 724+ detector using silicon double-crystal monochromated synchrotron radiation of wavelength 0.6889 Å on Beamline I19 at Diamond Light Source. Structures were solved by direct methods and developed by difference Fourier techniques using the SHELXTL[13] software package. The hydrogen atoms on the ligands were placed geometrically and refined using a riding model. The hydrogen atoms of coordinated water molecules could not be located but are included in the molecular formula and in values derived from it. The unit cell volume includes a large region of disordered solvent, which could not be modelled as discrete atomic sites. We employed PLATON/SQUEEZE[14] to calculate the contribution to the diffraction from the solvent region and thereby produced a set of solvent-free diffraction intensities. The final formula was calculated from elemental analysis data combined with TGA analysis: the contents of the solvent region are therefore included in the unit cell contents but not in the refinement model.

Crystal data for α-NOTT-220-solv: $[Bi_4(C_{16}H_6O_6)_3(H_2O)_4]\cdot(DMF)_7\cdot(H_2O)_6$; colourless chip (0.03×0.02×0.01 mm). *P*2/*c*, $a=19.567(6)$, $b=9.869(3)$, $c=22.135(6)$ Å, $\beta=104.81(1)^\circ$, $V=4132(2)$ Å^3, $Z=2$, $\rho_{calcd}=2.014$ g cm^{-3}, $\mu=8.591$ mm^{-1}, $F(000)=2420$. A total of 18307 reflections was collected, of which 9298 were unique giving $R_{int}=0.107$. Final R_1 (wR_2) = 0.0745 (0.185) with GOF = 0.80. The final difference Fourier extrema were 3.94 and −3.16 e Å^3.

Crystal data for β-NOTT-220-solv: $[Bi_4(C_{16}H_6O_6)_3(H_2O)_4]\cdot(DMF)_7\cdot(H_2O)_6$; colourless chip (0.03×0.02×0.01 mm). *P*2/*c*, $a=19.721(10)$, $b=9.862(5)$, $c=22.179(11)$ Å, $\beta=105.35(1)^\circ$, $V=4160(4)$ Å^3, $Z=2$, $\rho_{calcd}=2.001$ g cm^{-3}, $\mu=8.535$ mm^{-1}, $F(000)=2420$. A total of 26446 reflections was collected, of which 7290 were unique, giving $R_{int}=0.119$. Final R_1 (wR_2) = 0.0934 (0.273) with GOF = 1.04. The final difference Fourier extrema were 5.23 and −3.21 e Å^3.

CCDC-899427 (α-NOTT-220-solv) and CCDC-899428 (β-NOTT-220-solv) contain the supplementary crystallographic data for this paper. These data can be obtained free of charge from The Cambridge Crystallographic Data Centre via www.ccdc.cam.ac.uk/data_request/cif.

Modelling and simulations

Grand Canonical Monte Carlo (GCMC) simulations were performed using the MUSIC simulation suite[15] to calculate the adsorption of CH_4 and CO_2 molecules in NOTT-220a. The GCMC simulations involved 1.25×10^7 steps equilibration period followed by 1.25×10^7 steps production run for the methane uptake simulation, and 2×10^7 steps equilibration period followed by 2×10^7 steps production run for the CO_2 uptake simulation. The CH_4 molecule was described using a set of united-atom Lennard–Jones interaction parameters, $\sigma_O=3.73$ Å, $\varepsilon_O/k_B=148.0$ K, obtained from fitting to critical temperatures and saturated liquid densities.[16] The CO_2 mole-

cule was described using a force field, which quantitatively reproduces the vapour–liquid equilibrium (VLE) of the neat system and the binary mixtures. All three atoms of the CO_2 molecule were described as a set of united-atom Lennard–Jones interaction sites and described with the following parameters: $\sigma_O = 3.05$ Å, $\varepsilon_O/k_B = 79$ K for oxygen atoms, and $\sigma_C = 2.80$ Å, $\varepsilon_C/k_B = 27$ K for the carbon atom. A point charge of $+0.7$ was placed at the centre of mass of carbon atom and a point charge of -0.35 was placed at each oxygen atom, the C–O bond length taken to be 1.16 Å. All atoms in the MOF structure were described by an OPLS force field[17] with the exception of Bi atom, which was described by universal force field parameters,[18] and oxygen atoms, for which the force-field parameters were taken from a literature value.[19] The simulation supercell contained six ($2\times1\times3$) unit cells with periodic boundary conditions. The fugacity was calculated from the Peng–Robinson equation of state[20] and the MOF and the guest gas molecules were considered to be rigid. A Lennard–Jones potential was used to describe the van der Waals interactions with a cut-off distance of 14.0 Å.

Density functional theory (DFT) calculations were performed to derive the partial atomic charges subsequently used in the GCMC calculations and to calculate the binding energy of CH_4 and CO_2 to the binuclear Bi node. The DFT calculations were performed with the Q-Chem quantum chemistry package[21] using the B3LYP level of theory and the 6-31G* basis set and partial atomic charges were obtained using the ChelpG technique.[22] To determine the binding energy geometry optimisations were performed at the B3LYP/6-31G** level of theory, and the binding energies were subsequently calculated at the higher B3LYP/6-311++G** level as follows $BE = E(\text{complex}) - E(\text{linker}) - E_{opt}(CH_4)$.

Results and Discussion

Solvothermal reaction of H_4L (Scheme 1) and $Bi(NO_3)_3{\cdot}(H_2O)_5$ in a mixture of DMF/MeCN in the presence of piperazine and nitric acid at 100 °C for 10 h affords the solvated material NOTT-220-solv. In our hands, the addition of both piperazine and nitric acid in the synthesis is essential for the formation of NOTT-220-solv. In the absence of piperazine or nitric acid, NOTT-220-solv cannot be obtained or is formed together within an intractable mixture with other products. Single crystal diffraction data of NOTT-220-solv confirms that it crystallises in space group *P*2/*c* and has a neutral and non-interpenetrated structure constructed from binuclear $\{Bi_2\}$ centres bridged by tetracarboxylate ligands. Interestingly, the Bi^{III} centres in two solved crystal structures (denoted as α and β phases) have slightly altered coordination environments (Scheme 2). In both phases, each Bi^{III} ion is coordinated to three carboxylate groups from three different L^{4-} ligands (Bi–O = 2.280(12)–2.579(10) Å), and both Bi^{III} ions share three oxygen atoms from three bridging carboxylate groups (Bi–O = 2.481(10)–2.691(11) Å) to give irregular distorted pseudo-tetrahedral $[Bi_2(O_2CR)_6]$ nodes (Scheme 2). In addition, each node is coordinated to two water molecules. In the α phase, one water molecule resides on each Bi^{III} ion (Bi1–O13 = 2.582(12) Å, Bi2–O14 = 2.517(13) Å) to give a coordination number of eight for Bi1 and nine for Bi2. In the β phase, both water molecules reside on the same Bi^{III} ion, resulting in coordination numbers of nine for Bi1 and eight for Bi2 (Bi1–O13 = 2.659(12) Å, Bi1–O14 = 2.696(11) Å). Pairs of ligands at opposite sides of the node participate in an offset face-to-face π–π stacking interaction (perpendicular distance: 3.494(9) Å). If the $\{Bi_2\}$ node is considered as a singular 6-c vertex, and the ligand as two 3-c vertices, an overall 3,6-connected framework structure is formed having a new topology with a point symbol of $\{4{\cdot}6^2\}_2\{4^2{\cdot}6^5{\cdot}8^8\}\{6^2{\cdot}8\}$ according to the TOPOS database[23] (Figure 1). However, if the pair of π-stacked ligands is considered as one ligand, the topology of the structure simplifies to the **tfi** topology, with a point symbol of $\{6^2,8^4\}\{6^2,8\}$ (Figure S3 in the Supporting Information). In this analysis each ligand is regarded as two 3-connected nodes. However, if the ligand is considered as a single 4-connected node, the framework can be described as a 4,6-connected net with the point symbol $\{3^{12}.4^{24}.5^9\}$. Likewise, if the two π-stacked ligands are considered as one ligand, the topology simplifies to **pts** with the point symbol $\{4^2.8^2\}\{8^4\}$.

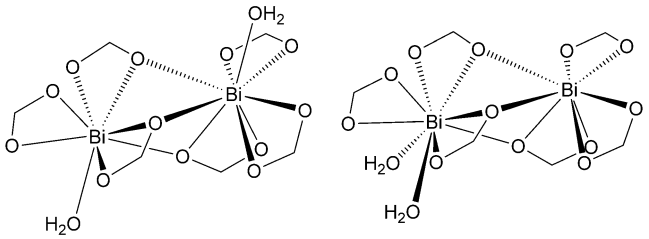

Scheme 2. a) Coordination geometry of α-NOTT-220-solv showing a water molecule bound to each Bi^{III} centre; b) coordination geometry of β-NOTT-220-solv showing two water molecules coordinated to the same Bi^{III} centre.

Due to the overall extended structure, the unit cell, space group and symmetry of the two phases of the material are identical and differ only by the position of one coordinated water molecule. The simulated PXRD patterns for the two phases are almost identical, and the experimental PXRD patterns are good matches with the simulated pattern, confirming the high purity of the bulk material (Figure S5 in the Supporting Information). Upon removal of the two coordinated water molecules on the $\{Bi_2\}$ node together with the solvent residing within the pores, the two desolvated phases are structurally identical.

The structure of NOTT-220-solv is highly porous, incorporating three distinct interconnected pore channels (denoted as *A*, *B*, *C*) by binding of the ligands to the $\{Bi_2\}$ nodes (Figure 2). Taking account of van der Waals radii, channel *A*, which is bound by phenyl rings and carboxylate oxygen atoms, has dimensions of 8.3×4.5 Å, while channel *B* is bound by Bi ions and hydrogen atoms from phenyl ring and has dimensions of 5.3×3.5 Å. Channel *C* (1.0×3.2 Å) is bound by Bi ions and phenyl rings. Although channel *C* is too narrow to allow guest diffusion, it is interconnected with channel *A*, and this allows the diffusion of the guest molecules into channel *C* via channel *A*. Channels *A*–*C* account for the 56% pore voids for this material as calculated by PLATON/SQUEEZE,[14] and are filled by free solvent molecules (DMF and water) which can be removed readily by heating in a flow of N_2 gas or under vacuum as confirmed by TGA (Figure S4 in the Supporting Information).

The acetone-exchanged sample, NOTT-220-acetone, was prepared to facilitate complete desolvation by suspending the as-synthesised NOTT-220-solv material in acetone for ten days

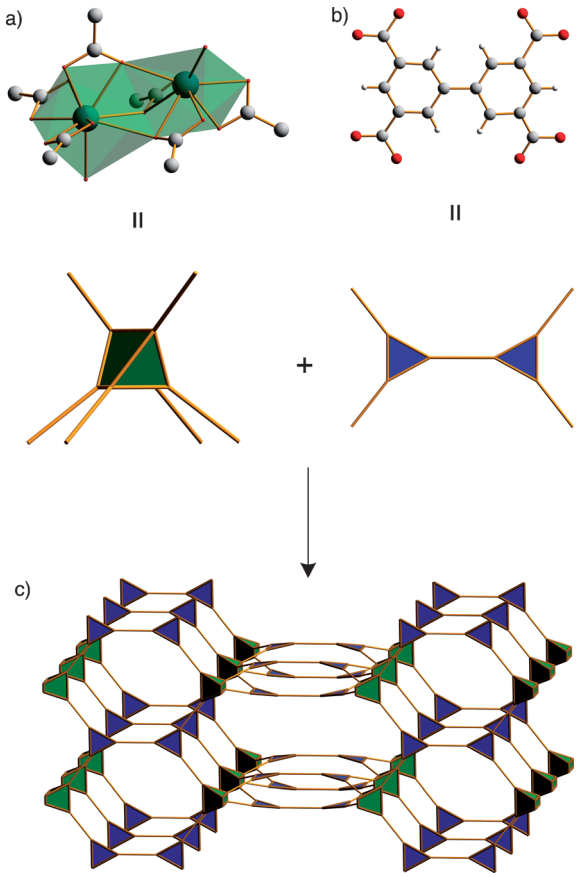

Figure 1. a), b) View of building blocks within NOTT-220-solv (C, grey; O, red; Bi, green). c) Assembly of building blocks into the idealised augmented net of $\{4{\cdot}6^2\}_2\{4^2{\cdot}6^5{\cdot}8^8\}\{6^2{\cdot}8\}$ point symbol.

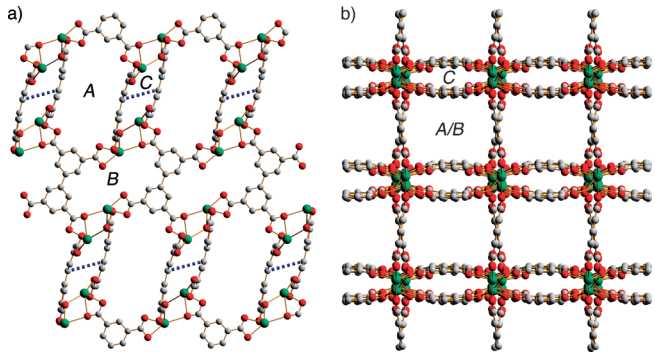

Figure 2. a) View of the crystal structure of NOTT-220-solv along the crystallographic *c* axis. The offset face-to-face π–π stacking (highlighted in blue) of the L^{4-} ligand is shown in channel *C*. b) View along the crystallographic [201] direction showing rectangular channels. Hydrogen atoms are omitted for clarity.

with frequent exchange of solvent. The fully desolvated material NOTT-220a was prepared by heating NOTT-220-acetone at 100 °C under reduced pressure (1×10^{-10} bar) for 24 h. The permanent porosity of NOTT-220a was confirmed by N_2 sorption isotherms at 77 K, which show reversible type-I adsorption behaviour (Figure 3a). Based on the N_2 isotherm, the apparent BET surface area of NOTT-220a was estimated to be 1014 m^2g^{-1}. The total micropore volume calculated from maximum N_2 uptake at saturation is 0.39 cm^3g^{-1}, consistent with the total crystallographically determined pore volume of 0.37 cm^3g^{-1} for both α- and β-forms. The pore volume and BET surface area of NOTT-220a are comparable to some of the light-metal-based MOFs (e.g., MIL-53(Al),[24] NOTT-300(Al)[25]), and are much higher than the values previously reported for heavy-metal-based MOFs (e.g., Bi-MOFs,[10a–c] U-MOFs,[26] Ba-MOFs[27]), but are lower than those of the most porous MOFs based on Zn^{II} or Cu^{II} ions.[4] Gravimetric H_2 adsorption isotherms at 77 K show good reversibility and an absence of hysteresis, and give a total storage capacity of 1.5 wt% at 1.0 bar and 2.8 wt% at 20 bar at 77 K (Figure 3b). This uptake is relatively low compared to high-performance H_2 storage materials,[6–8] but is consistent with the BET area and pore volume. The heat of adsorption is estimated to be 7.2 kJ mol^{-1} at zero surface coverage (Figure S8 in the Supporting Information), and is within the range (4–8 kJ mol^{-1}) typically observed for MOF materials.[1,2]

CO_2 and CH_4 sorption by NOTT-220a at 195 K shows type-I adsorption characteristics (Figure 3c, d). The maximum CO_2 uptake (47 wt% at saturation) was recorded at 195 K and 1.0 bar. At ambient temperatures, the CO_2 storage capacity of NOTT-220a was found to be 40.7 and 37.9 wt% at 273 and 293 K, respectively. The pore-size distribution, estimated from CO_2 adsorption data for NOTT-220a at 273 K, reveals four types of pores with diameters of 4.8, 5.4, 6.1 and 7.8 Å (Figure S6 in the Supporting Information). This is in excellent agreement with the measured channel diameters from the single-crystal structures (5–8 Å). The CH_4 uptakes at 20 bar were found to be 14.1 and 8.2 wt% at 195 and 293 K, respectively. The heats of adsorption at zero surface coverage for NOTT-220a are estimated to be 32 and 16 kJ mol^{-1} for CO_2 and CH_4 uptakes, respectively (Figure S8 in the Supporting Information), and are comparable to the values for MOF materials with similar uptakes.[1,2]

Desolvated NOTT-220a has a high bulk density (a crystallographically determined density) of 1.46 g cm^{-3} (framework-only density 3.17 g cm^{-3}) based upon removal of guest solvents and coordinated water molecules: this value is higher than those of other reported MOFs[4] with comparable or higher porosity and is due to the inclusion of $\{Bi_2\}$ nodes in the framework construction. The volumetric gas uptakes of NOTT-220a were determined based on the bulk density (1.46 g cm^{-3}) for the desolvated framework. The H_2 uptake of NOTT-220a at 20 bar and 77 K is 42 g L^{-1}, and is comparable to some of the high-performance MOFs,[4a–c] despite NOTT-220a having a much lower gravimetric uptake. At moderate pressure (20 bar) and ambient temperature (i.e., 293 K), the CO_2 uptake of NOTT-220a (553 g L^{-1}) is higher than that of MOF-210 and NU-100 (205 and 332 g L^{-1}, respectively),[4a,b] but is surpassed by NOTT-122[28a] (also noted as NU-125[28b] and NTU-105;[28c] 616 g L^{-1}), $[Cu_3(BTB)]$ (659 g L^{-1})[29] and USTA-20 (572 g L^{-1};[30] Table S2 in the Supporting Information). The maximum volumetric CH_4 uptake of NOTT-220a was determined to be 287 V(STP)/V at 195 K and 20 bar. At 293 K and 20 bar the corresponding CH_4 uptake drops to 165 V(STP)/V.

Significantly, these high uptakes of NOTT-220a are also confirmed by Grand Canonical Monte Carlo (GCMC) simulations,

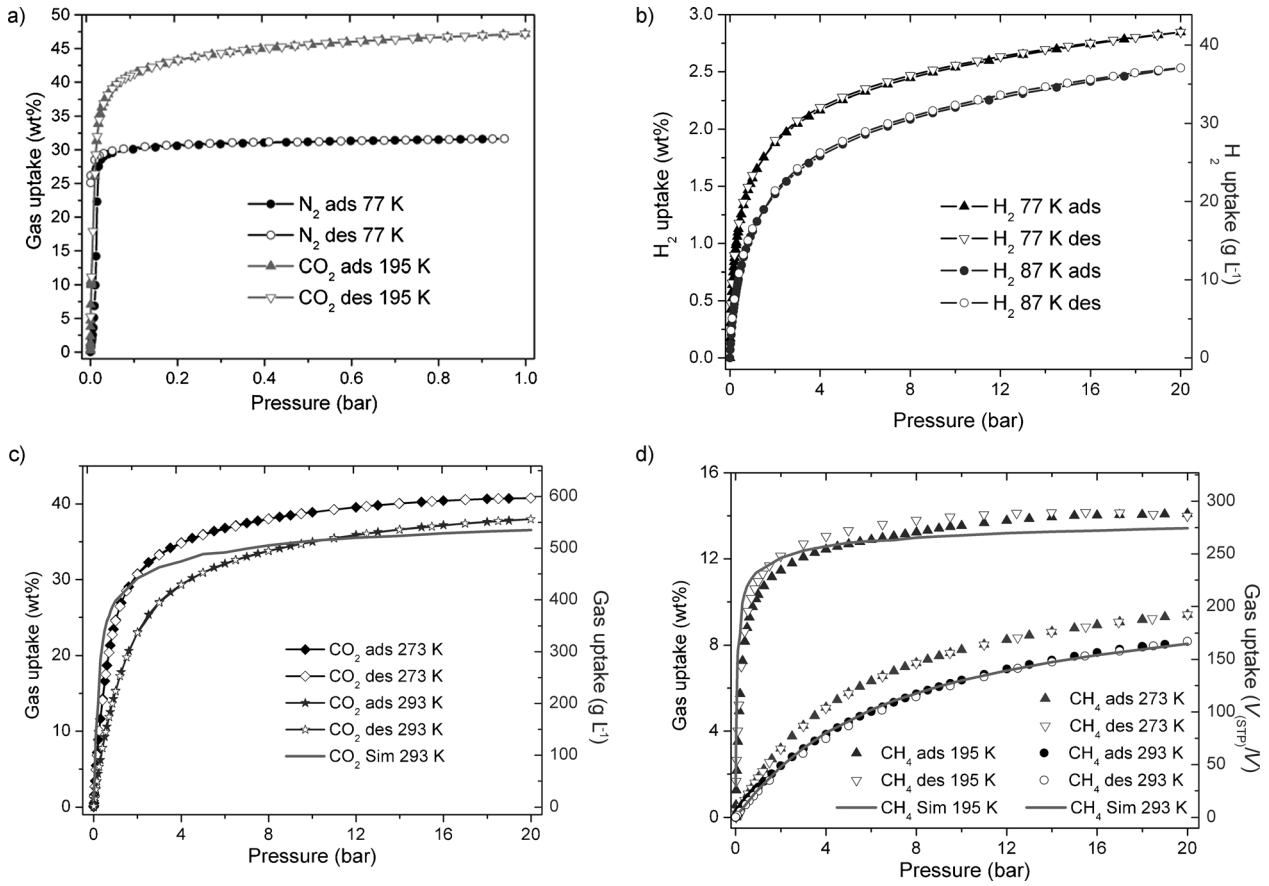

Figure 3. Gas adsorption isotherms for desolvated NOTT-220a. a) N_2 isotherms at 77 K and CO_2 isotherms at 195 K up to 1.0 bar; b) H_2 isotherms at 77 and 87 K up to 20 bar; c) CO_2 experimental and simulated isotherms at 273 and 293 K up to 20 bar; d) CH_4 experimental and simulated isotherms at 195, 273, and 293 K up to 20 bar.

which show excellent agreement with the experimental isotherm data, especially for CH_4 (Figure 3d). The discrepancy observed between simulated and experimental isotherms for CO_2 uptake is due to the lack of accuracy in describing the quadrupole moment of CO_2 molecule, which thus represents a challenge in these simulations. In addition, the preferred positions for adsorbed CH_4 and CO_2 within the framework host were predicted by DFT calculation to be above three oxygen atoms and one bismuth atom at the $\{Bi_2\}$ nodes (Figure S15 in the Supporting Information). The dominating interaction to stabilise CH_4 molecules is weak hydrogen bond between H atoms on CH_4 molecules and oxygen centres from carboxylate group (Figure S15a, b). In contrast, adsorbed CO_2 molecules form dipole interactions between the electropositive carbon centre and the oxygen centre from the carboxylate group (Figure S15c, d). An estimation of the binding energies of 8.1 kJ mol^{-1} for CH_4 and 21 kJ mol^{-1} for CO_2 was provided by the DFT calculations. Thus, the observed high uptake capacities and adsorption processes were fully modelled and confirmed from these GCMC and DFT simulations.

A CH_4 uptake of 189 V(STP)/V is obtained at 35 bar and 293 K from this modelling study (Figure S12 in the Supporting Information). Interestingly, this material, together with NOTT-122 (NU-125 and NTU-105),[28] Ni-, Co- and Mg-MOF-74,[2e,11] HKUST-1,[2e] NOTT-107,[9a,31] and PCN-14[2e,12] offer high volumetric CH_4 uptakes. Whereas most other MOF systems contain light transition metal ions, such as Cu^{II} or Ni^{II}, as nodes and thus have low framework densities, the incorporation of heavy metal ions (e.g., Bi in this study) into the MOF material could be potentially viable targets for volumetric gas storage. It is worth noting that the volumetric uptake capacities reported here represent the situation of MOFs in their single-crystal states and do not take into account any powder packing efficiency in the bulk materials, and therefore the working capacity at practical operation will be altered accordingly.

Conclusion

In summary, we have synthesised the porous NOTT-220-solv, based upon heavy Bi^{III} cations bridged by biphenyl-3,3′,5,5′-tetracarboxylate ligands. NOTT-220-solv incorporates a novel binuclear $\{Bi_2\}$ building block and exhibits a new framework topology due to the distorted coordination environment at $\{Bi_2\}$ centres. Although desolvated NOTT-220a exhibits an overall moderate porosity compared to a number of highly porous MOF materials (1014 m^2 g^{-1}), it shows good gravimetric gas uptakes, 40.7 and 37.9 wt% at 273 and 293 K for CO_2 and 14.1 and 8.2 wt% at 195 and 293 K for CH_4 at 20 bar. Furthermore, in spite of the high crystal density of the desolvated material high volumetric uptake capacities, particularly for CH_4 and CO_2 are

observed. Based upon this observation, we will further explore the synthesis of new highly porous MOFs based upon heavy metal ions, coupling high framework density with high porosity, and thus potentially achieving high volumetric gas uptakes.

Acknowledgements

S.Y. gratefully acknowledges receipt of a Leverhulme Trust Early Career Research Fellowship and a Nottingham Research Fellowship, and M.S. acknowledges receipt of an ERC Advanced Grant and EPSRC Programme Grant. E.B. acknowledges EPSRC Career Acceleration Fellowship, New Directions for EPSRC Research Leaders Award (EP/G005060) and ERC Starting Grant for funding. We are grateful to Diamond Light Source for the access to Beamline I19 and the EPSRC-funded National Crystallography Service for the collection of X-ray diffraction data.[32] We also thank Dr. Danil Dybtsev for helpful discussions.

Keywords: bismuth · CO_2 · grand canonical monte carlo simulations · metal–organic framework · methane

[1] R. J. Kuppler, D. J. Timmons, Q.-R. Fang, J.-R. Li, T. A. Makal, M. D. Young, D. Yuan, D. Zhao, W. Zhuang, H.-C. Zhou, *Coord. Chem. Rev.* **2009**, *253*, 3042 – 3066.

[2] a) L. J. Murray, M. Dincă, J. R. Long, *Chem. Soc. Rev.* **2009**, *38*, 1294 – 1314; b) X. Lin, N. R. Champness, M. Schröder, *Top. Curr. Chem.* **2009**, *293*, 35 – 76; c) K. Konstas, T. Osl, Y. Yang, M. Batten, N. Burke, A. J. Hill, M. R. Hill, *J. Mater. Chem.* **2012**, *22*, 16698 – 16708; d) T. A. Makal, J.-R. Li, W. Lu, H.-C. Zhou, *Chem. Soc. Rev.* **2012**, *41*, 7761 – 7779; e) J. A. Mason, M. Veenstra, J. R. Long, *Chem. Sci.* **2014**, *5*, 32 – 51.

[3] a) K. Sumida, D. L. Rogow, J. A. Mason, T. M. McDonald, E. D. Bloch, Z. R. Herm, T.-H. Bae, J. R. Long, *Chem. Rev.* **2012**, *112*, 724 – 781; b) J. M. Simmons, H. Wu, W. Zhou, T. Yildirim, *Energy Environ. Sci.* **2011**, *4*, 2177 – 2185.

[4] a) O. K. Farha, A. Özgür Yazaydın, I. Eryazici, C. D. Malliakas, B. G. Hauser, M. G. Kanatzidis, S. T. Nguyen, R. Q. Snurr, J. T. Hupp, *Nat. Chem.* **2010**, *2*, 944 – 948; b) H. Furukawa, N. Ko, Y. B. Go, N. Aratani, S. B. Choi, E. Choi, A. O. Yazaydin, R. Q. Snurr, M. O'Keeffe, J. Kim, O. M. Yaghi, *Science* **2010**, *329*, 424 – 428; c) Y. Yan, S. Yang, A. J. Blake, W. Lewis, E. Poirier, S. A. Barnett, N. R. Champness, M. Schröder, *Chem. Commun.* **2011**, *47*, 9995 – 9997; d) Y. Yan, I. Telepeni, S. Yang, X. Lin, W. Kockelmann, A. Dailly, A. J. Blake, W. Lewis, G. S. Walker, D. R. Allan, S. A. Barnett, N. R. Champness, M. Schröder, *J. Am. Chem. Soc.* **2010**, *132*, 4092 – 4094; e) H. Deng, S. Grunder, K. E. Cordova, C. Valente, H. Furukawa, M. Hmadeh, F. Gandara, A. C. Whalley, Z. Liu, S. Asahina, H. Kazumori, M. O'Keeffe, O. Terasaki, J. F. Stoddart, O. M. Yaghi, *Science* **2012**, *336*, 1018 – 1023.

[5] a) S. T. Zheng, Y. Li, T. Wu, R. A. Nieto, P. Feng, X. Bu, *Chem. Eur. J.* **2010**, *16*, 13035 – 13040; b) X. Liu, G. C. Guo, B. Liu, W. T. Chen, J. S. Huang, *Cryst. Growth Des.* **2005**, *5*, 841 – 843; c) X. Liu, G.-C. Guo, A.-Q. Wu, J.-S. Huang, *Inorg. Chem. Commun.* **2004**, *7*, 1261 – 1263.

[6] a) K. Sumida, M. R. Hill, S. Horike, A. Dailly, J. R. Long, *J. Am. Chem. Soc.* **2009**, *131*, 15120 – 15121; b) X. Luo, D. Luo, H. Zeng, M. Gong, Y. Chen, Z. Lin, *Inorg. Chem.* **2011**, *50*, 8697 – 8699; c) M. Kang, D. Luo, X. Luo, Z. Chen, Z. Lin, *CrystEngComm* **2012**, *14*, 95 – 97.

[7] a) D. Britt, H. Furukawa, B. Wang, T. G. Glover, O. M. Yaghi, *Proc. Natl. Acad. Sci. USA* **2009**, *106*, 20637 – 20640; b) M. Dincă, J. R. Long, *J. Am. Chem. Soc.* **2005**, *127*, 9376 – 9377.

[8] M. P. Suh, H. J. Park, T. K. Prasad, D.-W. Lim, *Chem. Rev.* **2012**, *112*, 782 – 835.

[9] a) X. Lin, I. Telepeni, A. J. Blake, A. Dailly, C. M. Brown, J. M. Simmons, M. Zoppi, G. S. Walker, K. M. Thomas, T. J. Mays, P. Hubberstey, N. R. Champness, M. Schröder, *J. Am. Chem. Soc.* **2009**, *131*, 2159 – 2171; b) W. Yang, A. Greenaway, X. Lin, R. Matsuda, A. J. Blake, C. Wilson, W. Lewis, P. Hubberstey, S. Kitagawa, N. R. Champness, M. Schröder, *J. Am. Chem. Soc.* **2010**, *132*, 14457 – 14469; c) S. Yang, S. K. Callear, A. J. Ramirez-Cuesta, W. I. F. David, J. Sun, A. J. Blake, N. R. Champness, M. Schröder, *Faraday Discuss.* **2011**, *151*, 19 – 36.

[10] a) A. Thirumurugan, W. Li, A. K. Cheetham, *Dalton Trans.* **2012**, *41*, 4126 – 4134; b) A. Thirumurugan, A. K. Cheetham, *Eur. J. Inorg. Chem.* **2010**, 3823 – 3828; c) A. C. Wibowo, S. A. Vaughn, M. D. Smith, H.-C. zur Loye, *Inorg. Chem.* **2010**, *49*, 11001 – 11008; d) M. Feyand, E. Mugnaioli, F. Vermoortele, B. Bueken, J. M. Dieterich, T. Reimer, U. Kolb, D. de Vos, N. Stock, *Angew. Chem.* **2012**, *124*, 10519 – 10522; *Angew. Chem. Int. Ed.* **2012**, *51*, 10373 – 10376; e) M. Feyand, M. Köppen, G. Friedrichs, N. Stock, *Chem. Eur. J.* **2013**, *19*, 12537 – 12546; f) V. Chandrasekhar, R. K. Metre, *Dalton Trans.* **2012**, *41*, 11684; g) A. C. Wibowo, M. D. Smith, J. Yeon, P. S. Halasyamani, H.-C. zur Loye, *J. Solid State Chem.* **2012**, *195*, 94 – 100.

[11] H. Wu, W. Zhou, T. Yildirim, *J. Am. Chem. Soc.* **2009**, *131*, 4995 – 5000.

[12] S. Ma, D. Sun, J. M. Simmons, C. D. Collier, D. Yuan, H.-C. Zhou, *J. Am. Chem. Soc.* **2008**, *130*, 1012 – 1016.

[13] G. M. Sheldrick, *Acta Crystallogr. Sect. A* **2008**, *64*, 112.

[14] A. L. Spek, *Acta Crystallogr. Sect. D* **2009**, *65*, 148.

[15] A. Gupta, S. Chempath, M. J. Sanborn, L. A. Clark, R. Q. Snurr, *Mol. Simul.* **2003**, *29*, 29 – 46.

[16] M. J. Martin, J. I. Siepmann, *J. Phys. Chem. B* **1998**, *102*, 2569 – 2577.

[17] W. L. Jorgensen, D. S. Maxwell, J. Tirado-Riveset, *J. Am. Chem. Soc.* **1996**, *118*, 11225 – 11236.

[18] A. K. Rappe, C. J. Casewit, K. S. Colwell, W. A. Goddard III, W. M. Skid, *J. Am. Chem. Soc.* **1992**, *114*, 10024 – 10035.

[19] Q. Yang, C. Zhong, *J. Phys. Chem. B* **2006**, *110*, 655 – 658.

[20] D.-Y. Peng, D. B. Robinson, *Ind. Eng. Chem. Fund.* **1976**, *15*, 59 – 64.

[21] Y. Shao, L. F. Molnar, Y. Jung, J. Kussmann, C. Ochsenfeld, S. T. Brown, A. T. B. Gilbert, L. V. Slipchenko, S. V. Levchenko, D. P. O'Neill, R. A. DiStasio, R. C. Lochan, T. Wang, G. J. O. Beran, N. A. Besley, J. M. Herbert, C. Y. Lin, T. Van Voorhis, S. H. Chien, A. Sodt, R. P. Steele, V. A. Rassolov, P. E. Maslen, P. P. Korambath, R. D. Adamson, B. Austin, J. Baker, E. F. C. Byrd, H. Dachsel, R. J. Doerksen, A. Dreuw, B. D. Dunietz, A. D. Dutoi, T. R. Furlani, S. R. Gwaltney, A. Heyden, S. Hirata, C. P. Hsu, G. Kedziora, R. Z. Khalliulin, P. Klunzinger, A. M. Lee, M. S. Lee, W. Liang, I. Lotan, N. Nair, B. Peters, E. I. Proynov, P. A. Pieniazek, Y. M. Rhee, J. Ritchie, E. Rosta, C. D. Sherrill, A. C. Simmonett, J. E. Subotnik, H. L. Woodcock, W. Zhang, A. T. Bell, A. K. Chakraborty, D. M. Chipman, F. J. Keil, A. Warshel, W. J. Hehre, H. F. Schaefer, J. Kong, A. Krylov, P. M. W. Gill, M. Head-Gordon, *Phys. Chem. Chem. Phys.* **2006**, *8*, 3172.

[22] C. M. Breneman, K. B. Wiberg, *J. Comput. Chem.* **1990**, *11*, 361 – 373.

[23] V. A. Blatov, *IUCr CompComm Newsletter* **2006**, *7*, 38 – 143.

[24] T. Loiseau, C. Serre, C. Huguenard, G. Fink, F. Taulelle, M. Henry, T. Bataille, G. Férey, *Chem. Eur. J.* **2004**, *10*, 1373 – 1382.

[25] S. Yang, J. Sun, A. J. Ramirez-Cuesta, S. K. Callear, W. I. F. David, D. P. Anderson, R. Newby, A. J. Blake, J. E. Parker, C. C. Tang, M. Schröder, *Nat. Chem.* **2012**, *4*, 887 – 894.

[26] a) J. Y. Kim, A. J. Norquist, D. O'Hare, *Dalton Trans.* **2003**, 2813 – 2814; b) C. Volkringer, I. Mihalcea, J.-F. Vigier, A. Beaurain, M. Visseaux, T. Loiseau, *Inorg. Chem.* **2011**, *50*, 11865 – 11867.

[27] M. L. Foo, S. Horike, Y. Inubushi, S. Kitagawa, *Angew. Chem.* **2012**, *124*, 6211 – 6215; *Angew. Chem. Int. Ed.* **2012**, *51*, 6107 – 6111.

[28] a) Y. Yan, M. Suyetin, E. Bichoutskaia, A. J. Blake, D. R. Allan, S. A. Barnett, M. Schröder, *Chem. Sci.* **2013**, *4*, 1731 – 1736; b) C. E. Wilmer, O. K. Farha, T. Yildirim, I. Eryazici, V. Krungleviciute, A. A. Sarjeant, R. Q. Snurr, J. T. Hupp, *Energy Environ. Sci.* **2013**, *6*, 1158 – 1163; c) X.-J. Wang, P.-Z. Li, Y. Chen, Q. Zhang, H. Zhang, X. X. Chan, R. Ganguly, Y. Li, J. Jiang, Y. Zhao, *Sci. Rep.* **2013**, *3*, 12012.

[29] B. Zheng, Z. Yang, J. Bai, Y. Li, S. Li, *Chem. Commun.* **2012**, *48*, 7025 – 7027.

[30] Z. Guo, H. Wu, G. Srinivas, Y. Zhou, S. Xiang, Z. Chen, Y. Yang, W. Zhou, M. O'Keeffe, B. Chen, *Angew. Chem.* **2011**, *123*, 3236 – 3239; *Angew. Chem. Int. Ed.* **2011**, *50*, 3178 – 3181.

[31] C. E. Wilmer, M. Leaf, C. Y. Lee, O. K. Farha, B. G. Hauser, J. T. Hupp, R. Q. Snurr, *Nat. Chem.* **2011**, *4*, 83 – 89.

[32] S. J. Coles, P. A. Gale, *Chem. Sci.* **2012**, *3*, 683 – 689.

Received: December 6, 2013
Revised: March 19, 2014
Published online on May 14, 2014